Natural Hazards
https://doi.org/10.1007/s11069-025-07402-0

ORIGINAL PAPER

Geomorphic thresholds for cascading hazards of debris flows and natural dam formation caused by large landslides

Hefryan Sukma Kharismalatri[1] · **Takashi Gomi**[2] · **Roy C. Sidle**[3]

Received: 26 August 2024 / Accepted: 22 May 2025

Abstract

This study investigates geomorphic thresholds that control cascading hazards initiated by large landslides (volume $> 10^5$ m^3), particularly their potential to generate natural dams or transform into debris flows. These two outcomes represent primary pathways in which large landslide debris interacts with channel networks, triggering downstream or upstream hazards. Using a global dataset of 188 large landslides, we analyzed key geomorphic parameters including inflow angle (entry angle of landslide into channel), local relief, and channel gradient. Our findings reveal distinct geomorphic thresholds: natural dams tend to form when landslides enter channels at inflow angles $> 60°$ and encounter channel gradients $< 10°$, while debris flows are more likely when inflow angles are $< 60°$ and channel gradients are $> 10°$. Power-law scaling exponents between landslide area and volume were lower for debris flows than for natural dam-forming landslides, reflecting differences in failure depth and mobility. While this study focuses on natural dam formation and debris flows as dominant hazard sequences, other outcomes such as channel infilling with sediment or partial blockage may occur depending on local topography and hydrological conditions. To avoid conflating past observations with future projections, we frame our results as empirical thresholds that help assess the potential for cascading impacts. These insights are particularly relevant for mountain communities in tectonically active regions where limited infrastructure, isolation, and steep terrain amplify hazard exposure. By identifying simple geomorphic thresholds associated with hazard transitions, this study provides a framework for improving risk assessment, early warning strategies, and land use planning to enhance hazard mitigation strategies and support evidence-based land use management.

Keywords Landslides · Debris flows · Natural dams · Sediment dynamics · Confluence angle · Cascading effects

✉ Takashi Gomi
gomit@agr.nagoya-u.ac.jp

[1] Institute of Global Innovation Research, Tokyo University of Agriculture and Technology, 3-5-8 Saiwai-cho, Fuchu, Tokyo 183-5809, Japan

[2] Graduate School of Bioagricultural Sciences, Nagoya University, Chikusa-ku, Furo-cho, Nagoya, Aichi 464-8601, Japan

[3] Mountain Societies Research Institute, University of Central Asia, 736000 Khorog, GBAO, Tajikistan

1 Introduction

Large and fast-moving landslides are significant forces in shaping landforms, triggered by either earthquakes or heavy precipitation (Larsen et al. 2010; Fan et al. 2020; Gong et al. 2021). Large landslides are defined as having volumes $> 10^5$ m^3 which move rapidly to channels (McColl and Cook 2024). Uplift rates, together with gravitational slope deformation that can precede and precondition the occurrence of large landslides that are influenced by both internal geological structure and hydrological pathways (Montgomery and Brandon 2002; Korup et al. 2007). These mass movements play a key role in spatial and temporal dynamics of sediment movement and landform evolution as they move from hillslopes to downstream channels (Gomi et al. 2002; Korup et al. 2010). Geomorphic processes, including sediment transport by cascading effects (i.e., a sequence of interconnected sediment movement by formation of temporary barriers, sediment deposition, channel realignment, and alterations in longitudinal connectivity by an initial landslide) induce extensive damage to mountain communities and infrastructure, with environmental changes persisting for centuries to millennia due to alterations in long-term sediment dynamics and budgets (Pearce and Watson 1986; Mani et al. 2023). Such cascading effects pose threats to food security and water resources management in mountainous regions around the world (Sidle et al. 2023; Maharjan et al. 2021).

Sediment from large landslides (volume $> 10^5$ m^3) can follow various geomorphic paths, including debris flows and natural dam formation, though other forms such as partial blockages may also occur (Kilburn and Pasuto 2003; Strom 2010). Debris flows resulting from large landslides exhibit high liquefaction, which facilitates rapid transport in steep channels and eventual deposition on downstream floodplains (Chen et al. 2006). Natural dams formed by landslides are a major hazard, obstructing river flows and creating impoundments that can cause upstream flooding and subsequent dam failure (Korup 2002). The sediment that forms natural dams is less mobile than that in long runout debris flows and is typically deposited in channels or near landslide-channel inflow points (confluences) where flow is restricted (Costa and Schuster 1988). Natural dams triggered by earthquakes and heavy rainfall are often clustered along mountain river systems (Strom 2010; Fan et al. 2014), reflecting preferential zones of valley constriction, fault-related slope instability, and sediment accumulation that influence long-term fluvial network evolution and valley morphology. Furthermore, natural dams pose a serious risk to downstream communities and infrastructure due to a potential rapid release of impounded water (Zheng et al. 2022). The legacy of large-scale sediment production driven by cascading effects in headwater regions can alter downstream sediment budgets for decades to centuries (Korup et al. 2010; Sidle et al. 2017).

Understanding the complex dynamics of large landslides is essential for identifying how landscape-scale geomorphic features govern landslide-driven sediment dynamics and long-term channel evolution in mountainous terrain. The size and frequency of landslides can be related to catchment morphology such as drainage density, headwater location, and channel junction angle (we hereafter call inflow angle) (Benda et al. 2004), as well as to the tendency of landslides to cluster in specific zones within a catchment, often due to underlying lithologic or structural controls (Densmore and Hovius 2000). Furthermore, because catchment drainage density and tributary inflow angles are associated with changes in the dominance of colluvial and fluvial processes (Hooshyar et al. 2017), both the magnitude and frequency of landslides, as well as their modes of interaction with main channels (e.g., natural dam formation), systematically vary across

different parts of catchment and channel network depending on geomorphic configuration (Abrahams, 1984; Ermini and Casagli, 2003; Liu and He, 2024). For instance, landslides in steep terrain of the Pacific Northwest, USA, deposited in channels with gradients $< 3.5°$ and inflow angles (i.e., angle between the landslide path and the receiving channel at the point of entry) $> 70°$, while deposition did not occur at acute inflow angles (Benda and Cundy 1990). Following a huge typhoon storm (1600 mm of rain in 72 h) on the Kii Peninsula of Japan in 2011, a series of landslides caused multiple natural dams that formed at inflow angles to streams $> 60°$ and channel gradients $< 10°$ (Kharismalatri et al. 2017). Because slope shape affects the accumulation of landslide materials (Xie et al. 2022), natural dam formation may be identified based on susceptibility of a given river reach to damming. The initiation of landslides in headwaters and the subsequent deposition and transport of sediment collectively contribute to sediment dynamics in catchments (Gomi et al. 2004; Yan et al. 2022) as well as channel morphology and aquatic ecosystems on decadal time scales (Ohira et al. 2021).

Quantifying patterns of debris flow occurrence and natural dam formation is essential for understanding where and how large-scale mass movements influence landscape-scale cascading effects and for developing regional disaster mitigation planning. Recent creation of global landslide databases helps to analyze landslide susceptibility and regional risk management (e.g., Fan et al. 2020; Yu et al. 2021; Kurilla and Fubelli 2022). For instance, Larsen et al. (2010) distinguished area–volume relationships between bedrock and soil-mantled landslides, showing that shallower, soil-mantled landslides with lower scaling exponents are more likely to evolve into debris flows. Differences such as landslide depth also affect the mobility of landslides in addition to the topographic conditions such as inflow angles of debris flows entering main channels (Imaizumi and Sidle 2007). Although many field investigations and laboratory experiments showed the timing and processes of debris flows (e.g., Chien-Yuan et al. 2005; Noviandi et al. 2022) or the formation and breaching of natural dams (e.g., Fan et al. 2020; Takayama and Imaziumi 2023), most studies focused separately on either debris flows or landslide dams and did not describe the processes and factors affecting these different hazard occurrences (Sidle et al. 2017). Because geomorphic connectivity from headwaters to downstream is important (Gomi et al. 2002), the combined effects of landslide propagation to either debris flows or natural dam formation in specific landscapes need to be fully identified to assess on-site landslide susceptibility and off-site cascading effects in river systems (Sidle et al. 2017; Sharma et al. 2023).

We hypothesize that the geomorphic parameters associated with large, rapid landslides in tectonically active regions, specifically slope geometry, landslide volume, and sliding surface depth, can reliably distinguish landslides that transition into debris flows from those resulting in natural dam formation, thereby serving as robust predictive criteria for hazard assessments, hazard mapping, mitigation strategies, and sustainable land use planning. Consequently, this study establishes criteria for understanding the occurrence of debris flows and the formation of natural dams arising from large, rapid landslides in tectonically active regions around the world such as Japan, Taiwan, New Zealand, China, Himalayas, Andes, Pacific Northwest of North America, and Tien Shan and Pamir Mountains of Central Asia. Drawing on our original global datasets of landslide occurrence, debris flows, and natural dam formation, the research underscores the importance of applying geomorphic information that differentiates debris flows from natural dams. This knowledge is also critical for both on-site and off-site hazard assessments, facilitating the development of hazard maps, mitigation measures, and sustainable land use planning in tectonically active landscapes.

2 Methodology

Information on large landslides, defined as having volumes > 10^5 m^3 or areas > 10^4 m^2, was collected from various journal publications, reports, and books (Supplementary Table S1). Because we focused on the large landslides, the number of cases of landslide dams and debris flows we collected was smaller than other comprehensive research on landslide dams (410 landslide dams by Fan et al. 2020) and debris flows (213 debris flows by Dowling and Santi 2014). Because large-scale landslides have also been defined as those with rapid and mixed movement of the collapsed material size more than 10^5 m^3 (McColl and Cook 2024), we included landslides defined as deep catastrophic landslides, deep-seated landslides, giant/huge/large landslides, rock avalanches, debris avalanches, catastrophic landslides, and long-runout landslides, while excluding slow-moving landslides such as earthflows that typically evolve gradually over long periods and are less likely to trigger rapid cascading effects such as debris flows or natural dam formation. "Natural dam" is defined as a natural blockage of a valley and channel by landslide material. Such dam-forming landslides are commonly triggered by excessive rainfall, earthquakes, and snow, glacier, and permafrost melt (Costa and Schuster 1988; Korup 2002; Strom 2010; Fan et al. 2020). Debris flows that occur on slopes and immediately mobilize downstream can initiate in a channel after long-term (i.e., seasonal to multi-year) deposition of landslide or other eroded material or they can initiate from landslide sediment that enters headwater channels and then immediately develops into a debris flow when the poorly sorted material becomes saturated or supersaturated (Sidle and Ochiai 2006).

Our methodology combined secondary data from a wide range of global literature with interpretive analysis using Digital Elevation Models (DEMs). For each large landslide, we extracted the following information, as available, from our surveys: coordinates, country, nearest city or town, date of landslide occurrence, and triggering factor. Because coordinates were not reported for most large landslides, we identified the locations of landslides using Google Earth and validated the locations using photographs or maps provided in publications. For each landslide, the dominant geology, landslide size (width, length, depth, area, and volume), dam size (width, length, height, and/or volume), and debris flow runout distance were summarized from publications. When landslide length and width were obtained from previous publications and our GIS analysis, landslide area was estimated by assuming a rectangular shape. This approach was adopted to address inconsistencies in data sources and to facilitate comparison with results reported in earlier studies. Landslide area (A_L) and volume (V_L) for natural dam formation and debris flows were examined using a scaling exponent γ in the volume versus area power law equation, $V_L = \alpha {A_L}^{\gamma}$, where α is the scaling factor that adjusts the magnitude of the relationship (Guzzetti et al. 2009; Larsen et al. 2010). When the year of landslide was identified, this was also recorded; if the year of landslide occurrence was not fully identified, we classified the relative age as "historic" or "prehistoric", where "historic" refers to landslides inferred to have occurred within the period of written or instrumental records, and "prehistoric" refers to older events identified only through geomorphic, sedimentary, or dating evidence.

Once the database of natural dams and debris flows was established, all landslide locations were overlaid on a 30-m digital elevation model (DEM) produced by the NASA Shuttle Radar Topography Mission (SRTM) with 1-arcsec data from the US Geological Survey Global Data Explorer (Farr et al. 2007). We measured local relief (Montgomery and Brandon 2002), inflow angle, and channel gradient (Kharismalatri et al. 2017) by GIS analysis of DEM data for each landslide. When the landslides and debris flows were within

a 5 km radius, local relief was estimated as the difference between the highest and lowest elevations within that radius (applicable to 83% of all landslides). For extremely large landslides—specifically those with lengths exceeding 2.5 km, we used a 10 km radius from the landslide center to calculate local relief (remaining 17% of the landslides). This is because a 5 km radius does not adequately capture the full elevational variation of such large-scale events and may lead to underestimation of actual relief. Expanding the analysis radius to 10 km ensures that the vertical extent of terrain is more accurately represented across landslides of varying spatial scales. We acknowledge that ideally, as suggested by Rickenmann (1999), local relief should be calculated along the landslide path, using the elevation difference between the scarp and toe. However, due to data limitations and inconsistencies in landslide delineation across sources, we adopted the radius-based approach as a standardized proxy to ensure comparability across the global dataset. We recognize that this may introduce some uncertainty, especially in complex terrain, and we note this as a limitation in interpreting relief-dependent trends. We estimated inflow angle, commonly expressed as confluence entry angle, as the planimetric angle between the landslide path to the channel and the receiving channel flow direction (Fig. 1). Channel gradient is the inclination of the channel in the reach where the landslide material was transported. We calculated channel gradient within a reach as four times the length of the landslide, with the landslide entry point positioned at the midpoint of the reach (Fig. 1). This approach ensured consistent characterization of the downstream geomorphic setting, although it introduces some dependence on landslide size. The length of the landslide was measured from the main scarp to its foot or landslide entry angle with the channel (i.e., inflow angle). Valley width was excluded because large landslides in our dataset ($> 10^5$ m^3) generally have sufficient momentum to traverse or block channels regardless of valley constriction, reducing its influence on sediment mobility.

To evaluate the statistical differences in geomorphic and topographic parameters between landslides that resulted in natural dam formation and those that evolved into debris flows, we conducted non-parametric Mann–Whitney U tests for each variable. This test is appropriate for comparing two independent groups when the assumption of normality is not met. We selected key parameters based on their relevance to post-failure sediment dynamics and hazard implications such as inflow angle (°), channel gradient (°), local relief

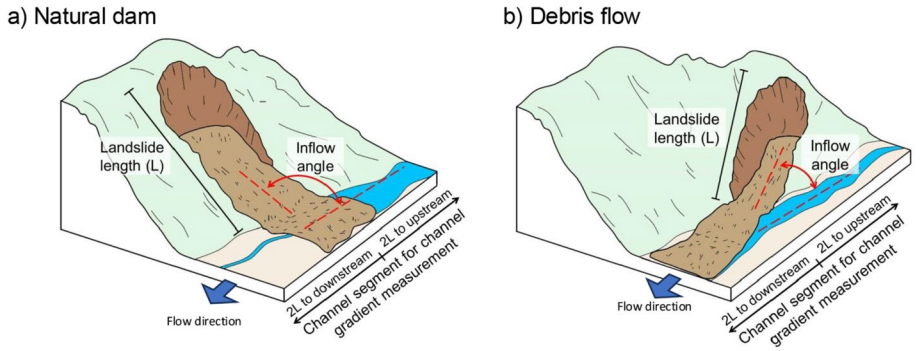

Fig. 1 Classification and measurement of **a** natural dams and **b** debris flows caused by large landslides. The channel gradient for each natural dam or debris flow was measured in a channel reach that was four times the length of the landslide with the entry point positioned in the middle (i.e., 2L upstream and 2L downstream)

(m), and landslide volume (m^3). To identify the possible geomorphic thresholds, we performed a binary logistic regression analysis to examine the influence of topographic conditions on debris flow occurrence and natural dam formation. The response variable was binary, coded as 1 for debris flow and 0 for natural dam formation. We used the two continuous explanatory variables of inflow angle (°) and channel gradient (°). Then, to evaluate the individual influence of topographic variables on debris flow occurrence, we conducted separate univariate logistic regression analyses using inflow angle (°) and channel gradient (°) as predictor variables. Prior to modeling, we removed records with missing values for either predictor. Multicollinearity was evaluated prior to analysis and no severe collinearity was detected for binary logistic regression. All statistical analyses were conducted in R (version R 4.5.0).

3 Results

We obtained data on 188 large landslides worldwide, focusing on their occurrence, regional distribution, and subsequent natural impacts such as debris flow and natural dam formation. Among them, 78% occurred from 1900 to 2018 (Table S1); 45% of the recorded landslides occurred after 2000, while 23% occurred from 1950 to 2000. Prehistoric and historic landslides constituted 20% of the records. Natural dams caused by large landslides formed in 124 of the cases, while 64 landslides progressed downstream as debris flows. These large landslides were reported in tectonically active areas around the Pacific Rim, Himalayas, central Europe, and Central Asia (Fig. 2). Of all the landslides, 47% occurred in East Asia (i.e., Japan, China, Taiwan; 38 natural dams and 29 debris flows) and Central Asia (i.e., Kyrgyzstan, Tajikistan, Kazakhstan; 21 natural dams and one debris flow). Large landslides in East Asia have been well documented during the past two decades due to the significant geomorphic and socio-economic impacts they have caused (Table S1, Fig. 2).

The main triggering factors of large landslides are earthquakes and hydrological processes attributed to heavy rainfall, permafrost thaw, or snow and glacial melt, which increase pore water pressure and, in the case of glacial retreat, reduce slope support at the toe (Fig. 3). The total volume of sediment produced by landslides ranged from 10^5 to 10^{10}

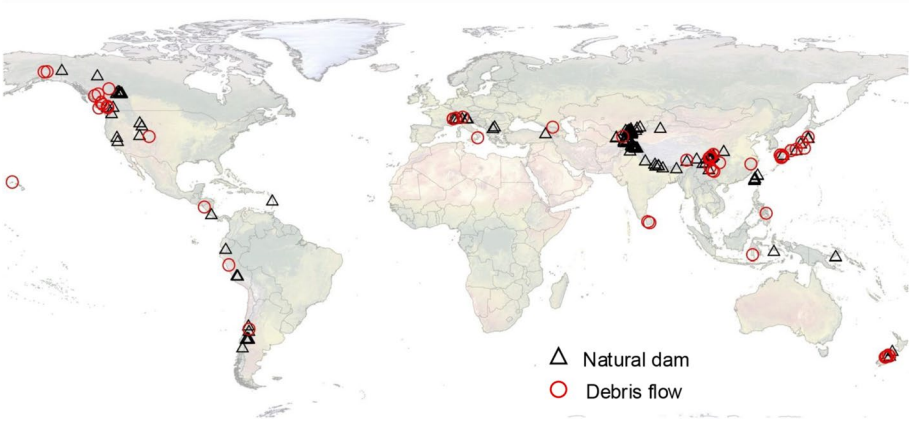

Fig. 2 Worldwide distribution of 188 natural dams and debris flows initiated by large landslides

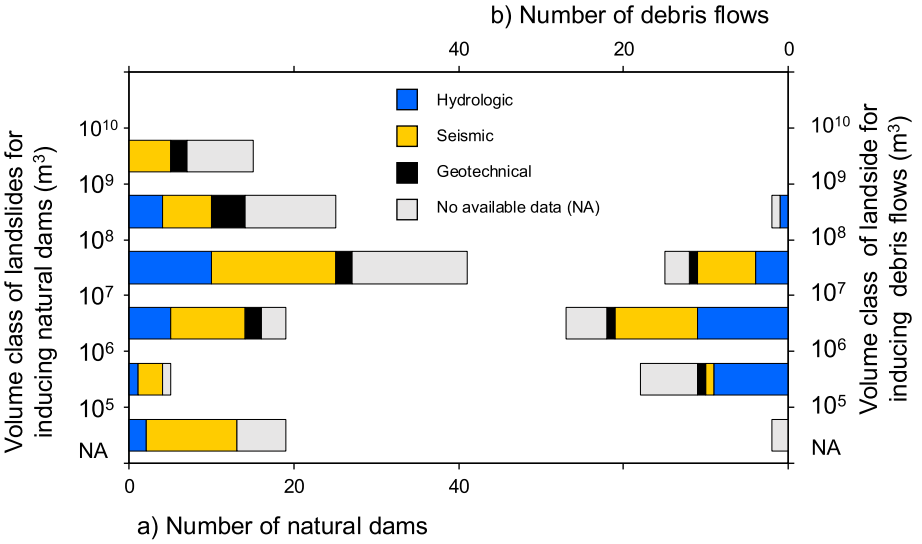

Fig. 3 Number of natural dams (**a**) and debris flows (**b**) by volume class and triggering factor. The volume of sediment produced by landslides was greater for those that formed natural dams than those that triggered debris flows

m^3. Among the landslides that formed natural dams, 65% were $> 10^7$ m^3. In contrast, the majority of debris flow–generating landslides were smaller, with 70% having volume $< 10^7$ m^3. These differences highlight the tendency for natural dams to be associated with larger-volume failures than debris flows (Fig. 3). Earthquake-generated natural dams had larger sediment volumes ($> 10^8$ m^3), and none of these larger landslides propagated downstream as debris flows. Large natural dams (10^8–10^9 m^3) occurred in tectonically active areas such as Chile, China, Central Asia, and the Himalayas. Most (80%) of the very large natural dams ($\geq 10^9$ m^3) occurred in Central Asia and the Hindu Kush Himalaya (Table S1). Volumes of landslides/debris flows triggered by hydrological processes had similar ranges compared to earthquake induced landslides, except for extremely large landslides (10^9–10^{10} m^3).

The area-volume relationships derived for large landslides that formed natural dams and those that initiated debris flows differed significantly and were influenced by the proximate mountainous terrain (Fig. 4). The relationship between landslide area and volume exhibited power-law scaling across five orders of magnitude from 10^4 to 10^9 m^2 in area and 10^5–10^{10} m^3 in volume (Fig. 4). Based on the relationship between volume and area using a power-law approximation, scaling exponents (γ) of all landslides, landslides that formed natural dams, and landslide that evolved into debris flows were 1.14, 1.14, and 0.79, respectively. Coefficients (α) of all landslides, landslides that formed natural dams, and those that evolved into debris flows were 3.93, 5.36, and 183.71, respectively.

Although landslides that evolved into debris flows appeared to show a steeper increase in volume with local relief (Fig. 5), statistical analysis (Mann–Whitney U-tests) revealed no significant difference in local relief between debris flow-generating landslides and those that formed natural dams. Debris flows generally occurred across a narrower volume range (10^5–10^8 m^3; Fig. 5). Approximately 59% of all landslides were in areas with mean local relief exceeding 1500 m, particularly in high-elevation regions such as the Himalayas, Tien

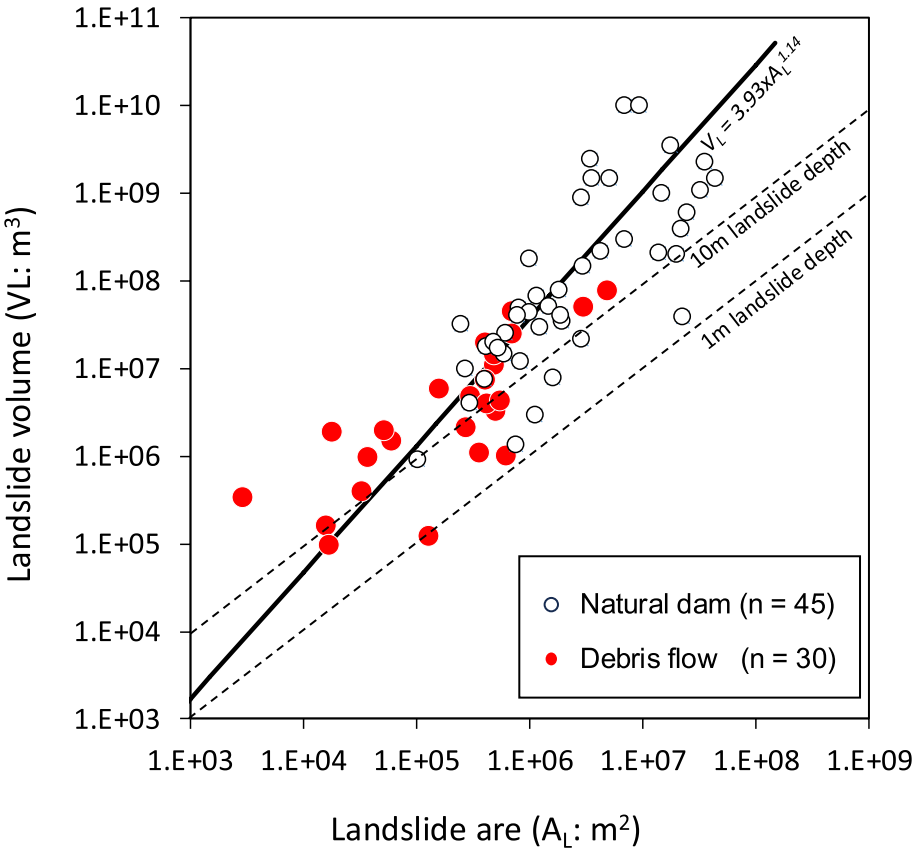

Fig. 4 Landslide area and volume relationship. Solid line indicates the equation based on Guzzetti et al. (2009). Break lines with 1 m and 10 m indicate theoretical depths of slide surfaces

Shan, Rocky Mountains, Carpathians, and Andes. Furthermore, more than 90% of very large landslides ($\geq 10^8$ m^3) occurred in areas with local relief greater than 1000 m and were associated with natural dam formation.

A binary logistic regression indicated that high channel gradient significantly increased the probability of debris flow occurrence (coefficient: 4.50, $p < 0.001$), while high inflow angle significantly decreased debris flow occurrence (coefficient: −4.50, $p < 0.001$). Inflow angles for landslides that formed natural dams ranged from 48° to 131° with a mean of 87° (standard deviation, SD = 19°; Fig. 6). In contrast, inflow angles for landslides that became downstream debris flows were considerably smaller, ranging from 1 to 80°, with a mean of 31° (SD = 20°). As inflow angle increased beyond approximately 60°, the probability of debris flow decreased markedly ($p < 0.01$), consistent with the threshold behavior identified in the logistic regression model (Fig. 7). This difference in inflow angle between the two groups was statistically significant ($p < 0.001$). Similarly, gradients of channels that landslides entered and propagated downstream as debris flows were larger (3°–36°) and more widely distributed than those where natural dams were formed (0.1°–10°; Figs. 6 and 7). Both logistic regression (Fig. 7) and Mann–Whitney U-test indicated that steeper channel gradients strongly favor debris flow mobilization ($p < 0.01$ for logistic regression and

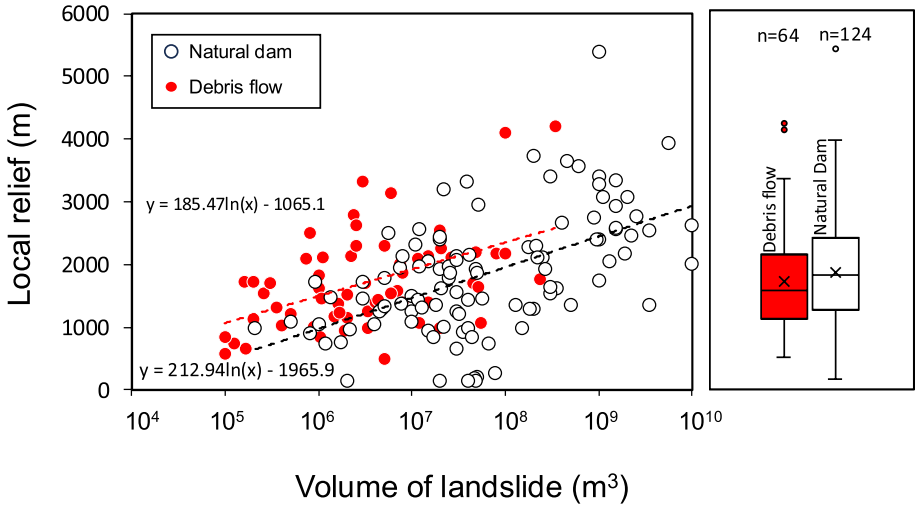

Fig. 5 Local relief and volumes of natural dams and debris flows triggered by large landslides. Boxes represent the interquartile range (IQR), spanning from the first quartile (Q1) to the third quartile (Q3). Lines inside the boxes indicate medians, and markers show mean values. Whiskers extend to the smallest and largest values within 1.5 times the IQR from Q1 and Q3. Outliers beyond this range are shown as individual points

$p < 0.001$ for U-test). Furthermore, seismically induced landslides were more likely to transition into debris flows when they occurred in steeper channel settings, compared to those triggered by rainfall (Fig. 8).

4 Discussion

The scaling exponents of landslides and transformation into debris flows or natural dams reveal crucial insights into the dynamics and behavior of these events. The scaling exponent in our power law equation ($\gamma = 1.14$) was lower than the exponent calculated by Guzzetti et al. (2009) from a broader range of 677 landslides, where the landslide area varied from several square meters to nearly 10^8 m^2 ($\gamma = 1.45$) (Fig. 4). Our exponent aligns more closely with the findings of Rice et al. (1969) in southern California ($\gamma = 1.11$) and Guthrie and Evans (2004) on Vancouver Island, British Columbia ($\gamma = 1.09$), both of which focused on relatively small landslides with areas up to 10^2 square meters. Similarly, Ju et al. (2023) calculated a comparable scaling exponent of 1.10 for 1326 landslides in Hong Kong, with sizes ranging from 10^1 to 10^3 square meters and γ values between 0.91 and 1.13, depending on the geological context. Topographic confinement and relief variability related to geological and geomorphic conditions may have affected the mobility and extent of landslide deposits, leading to different scaling relationships. Steeper and more confined settings tend to exhibit higher volume-to-area exponents due to enhanced runout efficiency.

Differences in power-law scaling exponents reveal distinct geomorphic and physical characteristics between landslides that formed natural dams and those that evolved into debris flows. When we differentiated landslides that formed natural dams from those that transformed into debris flows, the power law coefficient for debris flows was significantly lower ($\gamma = 0.79$) compared to that for natural dams ($\gamma = 1.14$). Guzzetti et al. (2009) also

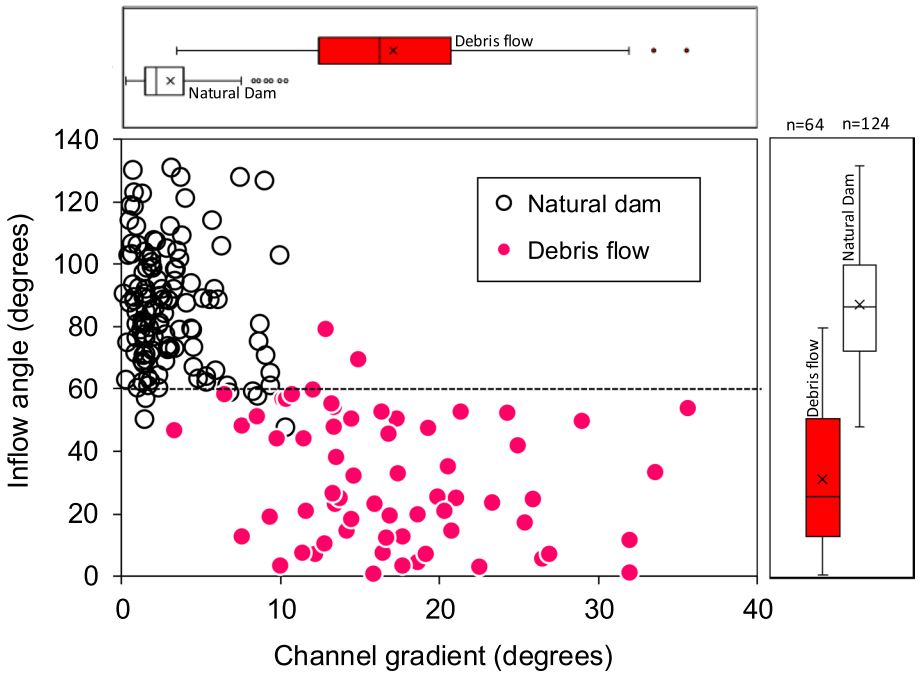

Fig. 6 Inflow angle versus channel gradient for the 188 large landslides segregated by those that deposited as natural dams in the channel and those that continued downstream as debris flows. Boxes represent the interquartile range (IQR), spanning from the first quartile (Q1) to the third quartile (Q3). Lines inside the boxes indicate medians, and markers show mean values. Whiskers extend to the smallest and largest values within 1.5 times the IQR from Q1 and Q3. Outliers beyond this range are shown as individual points. The 60° inflow angle indicates the likely threshold angle for the formation of natural dams versus debris flows by large landslides (also see analysis of logistic regression in Fig. 7)

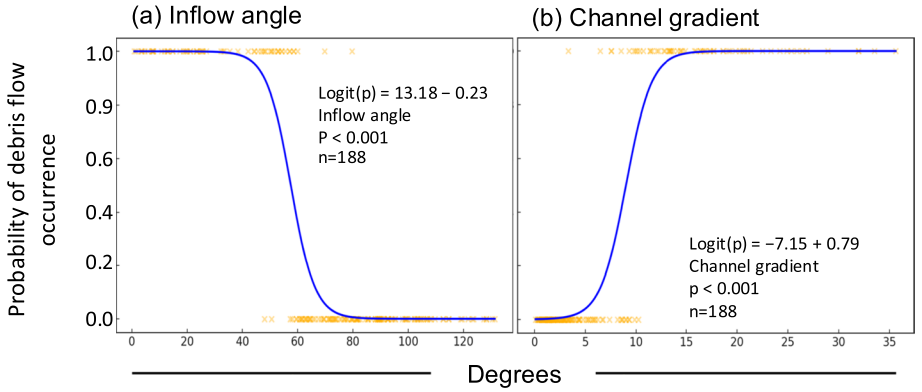

Fig. 7 Univariate logistic regression analyses using inflow angle (°) and channel gradient (°) as predictor variables of debris flow occurrence

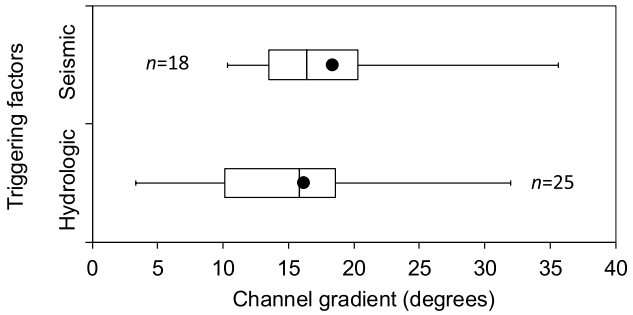

Fig. 8 Distribution of channel gradients for seismically and hydrologically induced debris flows. Left and right sides of boxes indicate upper and lower quantiles, respectively. Lines in boxes indicate mean values, while dots within boxes are median values. Bars on the outside of boxes indicate minimum and maximum values

derived power law exponents for landslides, many of which evolved into debris flows, using data from contrasting geographies like tropical Puerto Rico (Larsen and Torres Sanchez 1998) and the Queen Charlotte Islands, British Columbia (Martin et al. 2002). The scaling exponents for these regions were relatively small (0.898 and 0.880, respectively), closely matching the value we observed for larger landslides that transitioned into debris flows ($\gamma = 0.79$). These discrepancies in γ values across studies can be attributed to several factors such as lithologic and climatic differences (e.g., soil-mantled vs. bedrock terrain, rainfall dominated vs. dry climates) and variations in landslide size distributions and event types. For instance, the smaller exponent reported for soil-mantled landslides compared to bedrock failures (Larsen et al. 2010) reflects the tendency of shallow soils to liquefy more readily during intense rainfall or snowmelt. This process was consistent with our findings of possible mixing of displaced soil and water in steep channels, contributing to the mobilization of debris flow masses (Fig. 4). In contrast, landslides that formed natural dams often have deeper sliding surfaces, inferred from their higher ratio of landslide volume to surface area (Fig. 4). Because larger landslides tend to follow volume-dominated scaling, while smaller ones may be constrained by surface processes, a larger volume indicates a thicker deposit (i.e., a deeper sliding surface) for a given landslide surface area. Consequently, these larger volume failures with deep sliding surfaces are more likely to obstruct valleys and form natural dams. Because differences in volume estimation methods (e.g., empirical equations vs. mapped polygons) may also affect the area-volume relationship, future comparative studies that adopt standardized landslide classification and consistent measurement techniques are necessary to better capture the underlying physical processes driving landslides.

Our research identifies critical geomorphic thresholds using landslide entry (inflow angles) and drainage characteristics to determine whether large landslides lead to natural dam formation (Fig. 6; Fig. 7). We found that inflow angles $> 60°$, in combination with channel gradients $< 10°$, are significant factors in distinguishing between landslide dam formation and debris flow initiation (Figs. 6, 7). Further comparative analysis with findings from Strong and Mudd (2022) reveals that geometrically symmetric and gently sloping inflow angles predominantly occur in larger tributaries, contrasting with the sharp angles seen in smaller tributaries. These geometric features are indicative of the fundamental structural characteristics of river networks (Dunne 1980). For such

conditions, the momentum of the landslide sediment is significantly diminished when it impacts the valley sides or narrow valleys, causing extensive sediment deposition sufficient to obstruct the channel (Costa and Schuster 1988). Thus, potential for natural dam formation at a steeper angle (closer to perpendicular) increased due to sediment accumulation forming a blockage. Moreover, when the main channel gradient is $< 10°$, most of the sediment deposits at the slope base or in the channel bed due to the diminished transport capacity (Benda et al. 2005). Consequently, natural dam formation by large landslides was fundamentally governed by inflow angle and channel gradient, with confluence geometry acting as a critical threshold that facilitates sediment accumulation and channel blockage under conditions of reduced transport capacity.

Our findings align with the fundamental mechanics of debris flow initiation and mobility by large landslides. Low inflow angles ($< 60°$) enhance the alignment of gravitational and inertial forces along the channel direction, while steep channel gradients ($> 10°$) increase downslope acceleration and reduce basal friction, collectively facilitating rapid mass mobilization (Figs. 6, 7). Shallow inflow angles often occur in convergent hillslope geometries that promote flow into confined channels (Benda and Dunne 1997). Consequently, the majority (97%) of large landslides that produced debris flows had small inflow angles and steep channels due to the higher energy levels associated with less resistant pathways of incoming landsides entering channels. A study in the Pacific Northwest, USA, demonstrated that the transport capacity and deposition of debris flows were affected by topographic characteristics, where channel gradients greater than 3.5° and tributary inflow angles $< 70°$ facilitated deposition (Benda and Cundy 1990). Similarly, Brayshaw and Hassan (2009) found that 83% of landslides with inflow angles $\leq 40°$ in British Columbia resulted in debris flows, further supporting the impact of inflow dynamics. In a steep catchment in southern Nara Prefecture, Japan, many landslides directly evolved into debris flows with small hillslope-channel inflow angles (mostly $< 40°$), particularly in headwater reaches (Imaizumi and Sidle 2021). Additionally, flume experiments conducted under varying soil wetness conditions confirmed that more than 50% of landslide mass could transform into debris flows at low inflow angles (0° and 30°) in steep channels (15°) and propagate downstream (Kharismalatri et al. 2019). Findings of this flume study showed that debris flows resulting from large landslides exhibit high mobility and energy, and are strongly governed by hillslope-channel geometry, with low inflow angles enhancing flow alignment and steep channel gradients promoting gravitational acceleration and reduced basal friction—conditions that together facilitate rapid and sustained downslope motion.

Sediment mobility in landslides is strongly influenced by the triggering mechanism, particularly through its effects on soil–water content and initial gravitational forces. Landslides triggered by rainfall, glacial melt, or snowmelt are generally more prone to fluidization due to higher initial water content, although some earthquake-induced landslides can also mobilize rapidly under dry conditions (Fig. 8). The higher water content in these landslides enhances downstream transport, even in low-gradient channels. Typically, debris flows occur and accumulate in channels with gradients between 3° and 10° (Takahashi 2007), consistent with the behavior of water-induced debris flows observed in our study. In contrast, earthquake-triggered landslides, with lower water content, exhibit reduced mobility and often deposit upon reaching the main channel (Li et al. 2016; Koyanagi et al. 2020). Understanding these hydrological conditions is crucial for effective risk management and mitigation, as they inform the likelihood, timing, and potential mobility of landslides, enabling more accurate hazard forecasting and targeted early warning in regions vulnerable to diverse triggering events.

5 Conclusions

This study enhances the understanding of how large landslides initiate cascading geomorphic effects, particularly sediment-related hazard sequences such as natural dam formation or subsequent debris flows. We demonstrate that the inflow angle of landslides is closely associated with the likelihood of these cascading effects, supporting its relevance in the broader context of mountain landscape evolution (e.g., Campforts et al. 2022; Javidan et al. 2024). While previous research has highlighted the influence of geomorphic variables such as channel gradient and valley width, our findings show that a set of simple and measurable geomorphic thresholds can reliably distinguish between different post-failure outcomes of large landslides. These thresholds may serve as a useful screening tool for assessing sediment hazard potential in mountainous catchments. For example, in the event of a large upstream landslide, local authorities could use these simple geomorphic indicators to support a rapid, qualitative evaluation of whether natural dam formation or debris flow is more likely. Additionally, if a high-risk landslide area is mapped, these criteria can be used to inform potential mitigation measures. While integration with real-time data (e.g., rainfall or seismic activity) and operational early warning systems remains beyond the scope of this study, we view this threshold-based approach as a promising step toward more accessible, geomorphology-informed hazard assessments—particularly in remote or data-sparse high mountain regions. Its applicability in such settings makes it a promising tool for advancing community-based disaster preparedness and landscape-scale hazard management.

Supplementary Information The online version contains supplementary material available at https://doi.org/10.1007/s11069-025-07402-0.

Acknowledgements This study was supported by Global Innovative Research Institute of Tokyo University of Agriculture and Technology (TUAT, Japan. We appreciate Dr. Katsushige Shiraki, TUAT for variable comments in this study. We wish to thank for lab members of Watershed Hydrology and Ecosystem Management Laboratory, TUAT, Japan for support of data collection and advice on our research.

Author contributions HSK collected global information of landslides, analyzed data, and wrote the paper as the major contributor. TG organized and guided the study, developed analytical method, pointed out possible problems with the study, advised about solutions, and edited the paper. RCS pointed out possible problems with the study, advised about solutions, and edited the paper.

Funding Not applicable.

Availability of data and materials The dataset supporting the findings and conclusions of this article is included within the article as Supplemental Table S1.

Declarations

Conflict of interest The authors declare that they have no competing interests.

References

Abrahams AD (1984) Channel networks: a geomorphological perspective. Water Resour Res 20(2):161–188. https://doi.org/10.1029/WR020i002p00161

Benda LE, Cundy TW (1990) Predicting deposition of debris flows in mountain channels. Can Geotech J 27:409–417. https://doi.org/10.1139/t90-057

Benda L, Dunne T (1997) Stochastic forcing of sediment supply to the channel network from landsliding and debris flow. Water Resour Res 33(12):2849–2863. https://doi.org/10.1029/97WR02388

Benda LE, Poff NL, Miller D, Dunne T, Reeves G, Pess G, Pollock M (2004) The network dynamics hypothesis: how channel networks structure riverine habitats. Bioscience 54(5):413–427. https://doi.org/10.1641/0006-3568(2004)054[0413:TNDHHC]2.0.CO;2

Benda L, Hassan MA, Church M, May CL (2005) Geomorphology of steepland headwaters: the transition from hillslopes to channels. JAWRA J Am Water Resour as 41(4):835–851. https://doi.org/10.1111/j.1752-1688.2005.tb03773.x

Brayshaw D, Hassan MA (2009) Debris flow initiation and sediment recharge in gullies. Geomorphology 109:122–131. https://doi.org/10.1016/j.geomorph.2009.02.021

Campforts B, Shobe CM, Overeem I, Tucker GE (2022) The art of landslides: how stochastic mass wasting shapes topography and influences landscape dynamics. J Geophys Res Earth Surf 127(8):e2022JF006745. https://doi.org/10.1029/2022JF006745

Chen H, Dadson S, Chi YG (2006) Recent rainfall-induced landslides and debris flow in northern Taiwan. Geomorphology 77:112–125. https://doi.org/10.1016/j.geomorph.2006.01.002

Chien-Yuan C, Tien-Chien C, Fan-Chieh Y, Wen-Hui Y, Chun-Chieh T (2005) Rainfall duration and debris-flow initiated studies for real-time monitoring. Environ Geol 47:715–724. https://doi.org/10.1007/s00254-004-1203-0

Costa JE, Schuster RL (1988) The formation and failure of natural dams. Geol Soc Am Bull 100:1054–1068. https://doi.org/10.1130/0016-7606(1988)100%3c1054:TFAFON%3e2.3.CO;2

Densmore AL, Hovius N (2000) Topographic fingerprint of bedrock landslides. Geology 28:371–374. https://doi.org/10.1130/0091-7613(2000)28%3c371:TFOBL%3e2.0.CO;2

Dowling CA, Santi PM (2014) Debris flows and their toll on human life: a global analysis of debris-flow fatalities from 1950 to 2011. Nat Hazards 71:203–227. https://doi.org/10.1007/s11069-013-0907-4

Dunne T (1980) Formation and controls of channel networks. Prog Phys Geogr 4(2):211–239. https://doi.org/10.1177/030913338000400204

Ermini L, Casagli N (2003) Prediction of the behaviour of landslide dams using a geomorphological dimensionless index. Earth Surf Process Landf 28:31–47. https://doi.org/10.1002/esp.424

Fan X, Rossiter DG, van Westen CJ, Xu Q, Görüm T (2014) Empirical prediction of coseismic landslide dam formation. Earth Surf Process Landf 39(14):1913–1926. https://doi.org/10.1002/esp.3585

Fan X, Dufresne A, Subramanian SS, Strom A, Hermanns R, Stefanelli CT, Hewitt K, Yunus AP, Dunning S, Capra L, Geertsema M, Miller B, Casagli N, Jansen JD, Xu Q (2020) The formation and impact of landslide dams–State of the art. Earth-Sci Rev 203:103116. https://doi.org/10.1016/j.earscirev.2020.103116

Farr TG, Rosen PA, Caro E, Crippen R, Duren R, Hensley S, Kobrick M, Paller M, Rodriguez E, Roth L, Seal D, Shaffer S, Shimada J, Umland J, Werner M, Oskin M, Burbank D, Alsdorf D (2007) The shuttle radar topography mission. Rev Geophys 45(2):2005RG000183. https://doi.org/10.1029/2005RG000183

Gomi T, Sidle RC, Richardson JS (2002) Understanding processes and downstream linkages of headwater systems. Bioscience 52(10):905–916. https://doi.org/10.1641/0006-3568(2002)052[0905:UPADLO]2.0.CO;2

Gomi T, Sidle RC, Swanston DN (2004) Hydrogeomorphic linkages of sediment transport in headwater streams, Maybeso Experimental Forest, southeast Alaska. Hydrol Process 18(4):667–683. https://doi.org/10.1002/hyp.1366

Gong WP, Juang CH, Wasowski J (2021) Geohazards and human settlements: lessons learned from multiple relocation events in Badong, China-engineering geologist's perspective. Eng Geol 285:106051. https://doi.org/10.1016/j.enggeo.2021.106051

Guthrie RH, Evans SG (2004) Analysis of landslide frequencies and characteristics in a natural system, coastal British Columbia. Earth Surf Process Landf 29:1321–1339. https://doi.org/10.1002/esp.1095

Guzzetti F, Ardizzone F, Cardinali M, Rossi M, Valigi D (2009) Landslide volumes and landslide mobilization rates in Umbria, central Italy. Earth Planet Sci Lett 279(3–4):222–229. https://doi.org/10.1016/j.epsl.2009.01.005

Hooshyar M, Singh A, Wang D (2017) Hydrologic controls on junction angle of river networks. Water Resour Res 53(5):4073–4083. https://doi.org/10.1002/2016WR020267
Imaizumi F, Sidle RC (2007) Linkage of sediment supply and transport processes in Miyagawa Dam catchment, Japan. J Geophys Res Earth Surf. https://doi.org/10.1029/2006JF000495
Imaizumi F, Sidle RC (2021) Effects of terrain on the occurrence of debris flows after forest harvesting. Geogr Ann A Phys Geogr 103(3):259–272. https://doi.org/10.1080/04353676.2021.1932482
Javidan R, Rahmati O, Cerdà A, Escriva-Saneugenio F, Keesstra SD (2024) Spatial analysis of sediment connectivity and its applications. In Remote Sensing of Soil and Land Surface Processes. Elsevier. pp 369–383 https://doi.org/10.1016/B978-0-443-15341-9.00024-1
Ju LY, Zhang LM, Xiao T (2023) Power laws for accurate determination of landslide volume based on high-resolution LiDAR data. Eng Geol 312:106935. https://doi.org/10.1016/j.enggeo.2022.106935
Kharismalatri HS, Ishikawa Y, Gomi T, Shiraki K, Wakahara T (2017) Collapsed material movement of deep-seated landslides caused by Typhoon Talas 2011 on the Kii Peninsula, Japan. Int J Eros Control Eng 10:108–119. https://doi.org/10.13101/ijece.10.108
Kharismalatri HS, Ishikawa Y, Gomi T, Sidle RC, Shiraki K (2019) Evaluating factors for controlling sediment connectivity of landslide materials: a flume experiment. Water 11:w11010017. https://doi.org/10.3390/w11010017
Kilburn CR, Pasuto A (2003) Major risk from rapid, large-volume landslides in Europe (EU Project RUNOUT). Geomorphology 54:3–9. https://doi.org/10.1016/S0169-555X(03)00050-3
Korup O (2002) Recent research on landslide dams-a literature review with special attention to New Zealand. Prog Phys Geogr 26(2):206–235. https://doi.org/10.1191/0309133302pp333ra
Korup O, Clague JJ, Hermanns RL, Hewitt K, Strom AL, Weidinger JT (2007) Giant landslides, topography, and erosion. Earth Planet Sci Lett 261:578–589. https://doi.org/10.1016/j.epsl.2007.07.025
Korup O, Densmore AL, Schlunegger F (2010) The role of landslides in mountain range evolution. Geomorphology 120(1–2):77–90. https://doi.org/10.1016/j.geomorph.2009.09.017
Koyanagi K, Gomi T, Sidle RC (2020) Characteristics of landslides in forests and grasslands triggered by the 2016 Kumamoto Earthquake. Earth Surf Process Landf 45:893–904. https://doi.org/10.1002/esp.4781
Kurilla LJ, Fubelli G (2022) Global debris flow susceptibility based on a comparative analysis of a single global model versus a continent-by-continent approach. Nat Hazards 113(1):527–546. https://doi.org/10.1007/s11069-022-05313-y
Larsen MC, Torres Sanchez AJ (1998) The frequency and distribution of recent landslides in three montane tropical regions of Puerto Rico. Geomorphology 24:309–331. https://doi.org/10.1016/S0169-555X(98)00023-3
Larsen IJ, Montgomery DR, Korup O (2010) Landslide erosion controlled by hillslope material. Nat Geosci 3:247. https://doi.org/10.1038/ngeo776
Li G, West AJ, Densmore AL, Hammond DE, Jin Z, Zhang F, Wang J, Hilton RG (2016) Connectivity of earthquake-triggered landslides with the fluvial network: Implications for landslide sediment transport after the 2008 Wenchuan earthquake. J Geophys Res Earth Surf 121:703–724. https://doi.org/10.1002/2015JF003718
Liu W, He S (2024) Influence of runoff on debris flow propagation at a catchment scale: a case study. Landslides 21:1757–1774. https://doi.org/10.1007/s10346-024-02255-3
Maharjan SB, Steiner JF, Shrestha AB, Maharjan A, Nepal S, Shrestha MS, Bajracharya B, Rasul G, Shrestha M, Jackson M, Gupta N (2021) The Melamchi flood disaster: Cascading hazard and the need for multihazard risk management. Kathmandu, Nepal: ICIMOD
Mani P, Allen S, Evans SG, Kargel JS, Mergili M, Petrakov D, Stoffel M (2023) Geomorphic process chains in high-mountain regions- a review and classification approach for natural hazards assessment. Rev Geophys 61(4):e2022RG000791. https://doi.org/10.1029/2022RG000791
Martin Y, Rood K, Schwab JW, Church M (2002) Sediment transfer by shallow landsliding in the Queen Charlotte Islands, British Columbia. Can J Earth Sci 39(2):189–205. https://doi.org/10.1139/e01-068
McColl ST, Cook SJ (2024) A universal size classification system for landslides. Landslides 21(1):111–120. https://doi.org/10.1007/s10346-023-02131-6
Montgomery DR, Brandon MT (2002) Topographic controls on erosion rates in tectonically active mountain ranges. Earth Planet Sci Lett 201:481–489. https://doi.org/10.1016/S0012-821X(02)00725-2
Noviandi R, Gomi T, Kharismalatri HS, Sidle RC, Ritonga RP, Shiraki K (2022) The mobility of landslides in pumice: insights from a flume experiment. Water 14(19):3083. https://doi.org/10.3390/w14193083
Ohira M, Watanabe Y, Gomi T, Sakai M (2021) Long-term impacts of forest disturbances: Comparing cumulative effects of clearcut logging versus landslide on stream conditions and abundance of a headwater stonefly *Scopura montana*. Freshw Biol 66(10):2004–2015. https://doi.org/10.1111/fwb.13811

Pearce AJ, Watson AJ (1986) Effects of earthquake-induced landslides on sediment budget and transport over a 50-yr period. Geology 14:52–55. https://doi.org/10.1130/0091-7613(1986)14%3c52:EOELOS%3e2.0.CO;2

Rice RM, Corbett ES, Bailey RG (1969) Soil slips related to vegetation, topography, and soil in Southern California. Water Resour Res 5(3):647–659. https://doi.org/10.1029/WR005i003p00647

Rickenmann D (1999) Empirical relationships for debris flows. Nat Hazards 19:47–77. https://doi.org/10.1023/A:1008064220727

Sharma S, Talchabhadel R, Nepal S, Ghimire GR, Rakhal B, Panthi J, Adhikari BR, Pradhanang SM, Maskey S, Kumar S (2023) Increasing risk of cascading hazards in the central Himalayas. Nat Hazards 119(2):1117–1126. https://doi.org/10.1007/s11069-022-05462-0

Sidle RC, Gomi T, Usuga JCL, Jarihani B (2017) Hydrogeomorphic processes and scaling issues in the continuum from soil pedons to catchments. Earth-Sci Rev 175:75–96. https://doi.org/10.1016/j.earscirev.2017.10.010

Sidle RC, Khan AA, Caiserman A, Qadamov A, Khojazoda Z (2023) Food security in high mountains of Central Asia: a broader perspective. Bioscience 73(5):347–363. https://doi.org/10.1093/biosci/biad025

Sidle R, Ochiai H (2006) Processes, prediction, and land use. Water resources monograph 18 American Geophysical Union, Washington 525. p 312. https://doi.org/10.1029/WM018

Strom A (2010) Landslide dams in Central Asia region. J Jpn Landslide Soc 47:309–324. https://doi.org/10.3313/jls.47.309

Strong CM, Mudd SM (2022) Explaining the climate sensitivity of junction geometry in global river networks. Proc Natl Acad Sci U S A 119(50):e2211942119. https://doi.org/10.1073/pnas.2211942119

Takahashi T (2007) Debris flow: mechanics, prediction and countermeasures. Taylor & Francis 572.

Takayama S, Imaizumi F (2023) Effects of coarse particles on downstream face erosion processes and outflow discharge during the overtopping of a landslide dam. Landslides 20(2):351–366. https://doi.org/10.1007/s10346-022-01973-w

Xie X, Wang X, Zhao S, Li Z, Qin X, Xu S (2022) Experimental study on the accumulation characteristics and mechanism of landslide debris dam. Front Earth Sci 10:878782. https://doi.org/10.3389/feart.2022.878782

Yan X, Jiao J, Li M, Qi H, Liang Y, Xu Q, Zhang Z, Jiang X, Li J, Zhang Z, Wang H (2022) Lateral sediment connectivity of landslides occurred under a heavy rainstorm and its influence on sediment yield of slope-channel cascade on the loess plateau. CATENA 216:106378. https://doi.org/10.1016/j.catena.2022.106378

Yu GA, Yao W, Huang HQ, Liu Z (2021) Debris flows originating in the mountain cryosphere under a changing climate: a review. Prog Phys Geog Earth Environment 45(3):339–374. https://doi.org/10.1177/0309133320961705

Zheng H, Shi Z, Peng M, Guan S, Hanley KJ, Feng S (2022) Amplification effect of cascading breach discharge of landslide dams. Landslides 19(3):573–587. https://doi.org/10.1007/s10346-021-01816-0